Modelling of gyration effects on jets in crossflow

Franck Mastrippolito, Rémi Manceau, Pascal Bruel

Applied Mathematics Departement
Inria-Cagire group
CNRS–University of Pau
Pau, France

Journée thématique SFT
Aérothermique des systèmes propulsifs pour l'aéronautique
Paris, 20 octobre 2022

Introduction

✓ European project SOPRANO

✓ Collaboration ONERA Toulouse/LMAP: effects of gyration on effusion cooling

✓ Experiments (ONERA) and second-moment RANS simulations (LMAP)

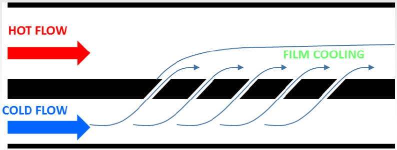

✓ Challenges

- ▷ Complex physics: jet/boundary layer interaction with gyration, and jet/jet interactions
- ▷ Importance of the wall/turbulence interaction for heat transfer

✓ Questions:

- ▷ Is the second-moment closure (EB-RSM) sufficiently robust for this type of problems
- ▷ Accuracy? Superiority to standard eddy-viscosity models?

✓ Mid-term objective: proposing a reliable and low-cost approach

- ▷ Parametric studies
- ▷ Develop homogeneous or heterogeneous boundary conditions for industrial computations and/or LES

Outline of the presentation

- ✓ Experimental configuration
- ✓ Simulations
  - ▷ Presentation of the EB-RSM
  - ▷ Comparison with experiments
- ✓ Ongoing work
  - ▷ Presentation of the hybrid RANS-LES approach (HTLES)
  - ▷ Some illustrative results

Configuration

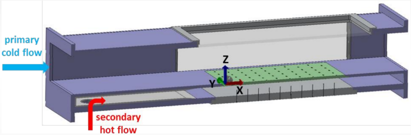

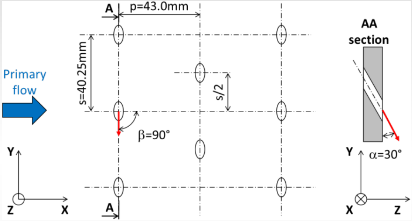

- ✓ Geometry:
  - ▷ 10 rows of 9 holes in staggered arrangement. Diameter $D = 5$ mm.
  - ▷ Pitch angle α =30°. Yaw angle $\beta = 90°$ (gyration).
  - ▷ Spacing: $s = 8.05D$ and $p = 8.6D$
- ✓ Flows:
  - ▷ Main: 3.39 m s^{-1} ($Re_p = 45500$)
  - ▷ Secondary 2.88 m s^{-1} ($Re_s = 10400$)
  - ▷ Leads to 26 m s^{-1} inside the holes: $V_j/V_p = 7.88$
  - ▷ Momentum flux ratio $I = \rho_j V_j^2 / \rho_p V_p^2 = 58.2$

Experimental database

- ✓ Velocity measured by stereo-PIV

  - ▷ Horizontal planes at $z/D = 1.16; 2.36; 3.96; 5.26; 6.96; 8.36$

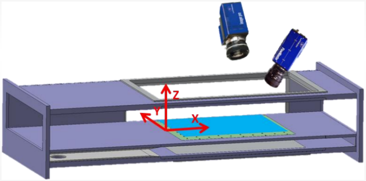

  - ▷ Vertical planes at constant x through the first 4 rows and inter-rows

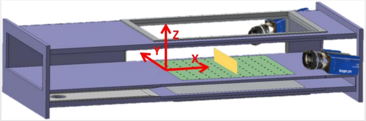

- ✓ Temperature field: cold wires

- ✓ Surface temperatures: infrared thermography

Presentation of the simulations

✓ Open-source code Code_Saturne developed by EDF (Archambeau et al., 2004)

✓ RANS models: EB-RSM and k-ω-SST for comparison

✓ Structured mesh generated with Gmsh by duplication of the 1-hole pattern

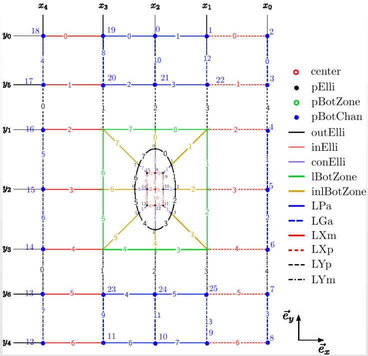

✓ Refined near-wall mesh ($y^+ = 1$ criterion), geometric expansion

✓ Grid convergence checked (4 grid levels). Results plotted for 70×10^6 cells

Presentation of the simulations

✓ Experimental profile available in the boundary layer at $3.05D$ upstream of the first row (location $x = 0$)

✓ Generation of the inlet conditions:

- ▷ Precursor simulation of a developing boundary layer
- ▷ Extraction of the profile corresponding to the correct boundary layer thickness
- ▷ Make possible the injection at the inlet of all the variables of the model (velocities, Reynolds stresses, dissipation)

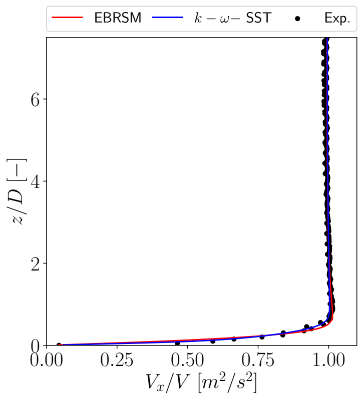

Second-moment closure EB-RSM

✓ Eddy-viscosity models: $\overline{u_i u_j} = -2\nu_t S_{ij} + \dfrac{2}{3} k \delta_{ij}$

✓ Second-moment closures (RSM): Reynolds-stress transport equations

$$\frac{\mathrm{d}\overline{u_i u_j}}{\mathrm{d}t} = \underbrace{\nu \frac{\partial^2 \overline{u_i u_j}}{\partial x_k \partial x_k}}_{D^{\nu}_{ij}} \underbrace{- \frac{\partial \overline{u_i u_j u_k}}{\partial x_k}}_{D^{T}_{ij}} \underbrace{- \frac{1}{\rho}\overline{u_i \frac{\partial p}{\partial x_j}} - \frac{1}{\rho}\overline{u_j \frac{\partial p}{\partial x_i}}}_{\phi^{*}_{ij}}$$

$$\underbrace{- \overline{u_i u_k}\frac{\partial U_j}{\partial x_k} - \overline{u_j u_k}\frac{\partial U_i}{\partial x_k}}_{P_{ij}} - \underbrace{2\nu \overline{\frac{\partial u_i}{\partial x_k}\frac{\partial u_j}{\partial x_k}}}_{\varepsilon_{ij}}$$

✓ Influence of the wall: nonlocal blockage effect $\Rightarrow$ two-component limit

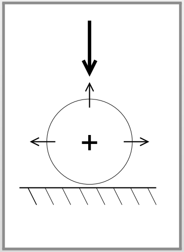

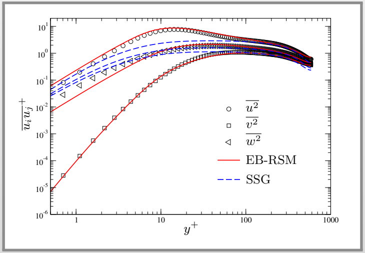

Second-moment closure EB-RSM

- ✓ Elliptic relaxation (Durbin) : $(1 - L^2\nabla^2)\dfrac{\phi^*_{ij}}{\lambda} = \dfrac{\phi^h_{ij}}{\lambda}$ $\Rightarrow$ 6 additional equations, unstable
- ✓ Elliptic blending: $\left|\begin{array}{l}(1 - L^2\nabla^2)\alpha = 1\\ \phi^*_{ij} = (1-\alpha^3)\phi^w_{ij} + \alpha^3\phi^h_{ij}\end{array}\right.$
- ✓ Taylor series expansion

$$\Rightarrow \boxed{\phi^w_{ij} = -5\frac{\varepsilon}{k}\left[\overline{u_i u_k} n_j n_k + \overline{u_j u_k} n_i n_k - \frac{1}{2}\overline{u_k u_l} n_k n_l \left(n_i n_j + \delta_{ij}\right)\right]}$$

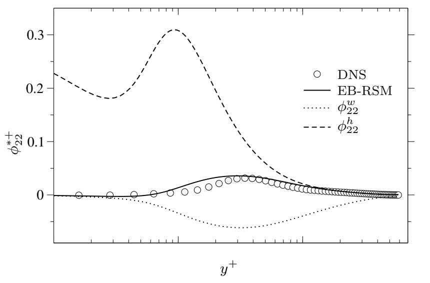

EB-RSM: examples of applications

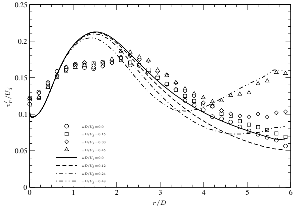

Cooling of a gaz turbine disk by an impinging jet
(Manceau et al., 2014)

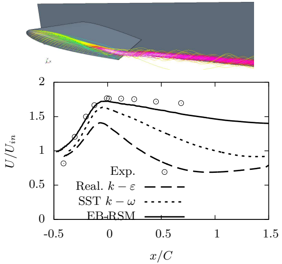

Wake of NACA 0012
(Lardeau and Manceau, 2014)

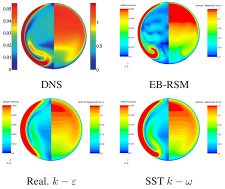

Flow in a curved pipe
(Lardeau and Manceau, 2014)

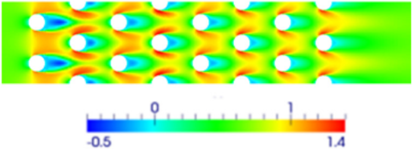

Turbine blade cooling: pin fins
(Benhamadouche et al., 2020)

GGDH model $\overline{u_i\theta} = -C_\theta \frac{k}{\varepsilon}\overline{u_i u_k}\frac{\partial T}{\partial x_x}$

is sufficient for forced convection

Applications by other groups

Compressor blades

(Borello et al., 2005)

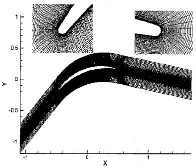

Fig. 10 DCA cascade—computational mesh (coarse discretization)

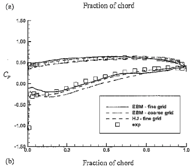

Fig. 11 DCA cascade—C_p distribution: (a) HJ simulations and (b) EBM simulations

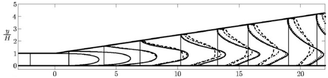

Control by vortex generators
(Törnblom and Johansson, 2007)

Assemblage combustible

(Dovizio et al., 2019)

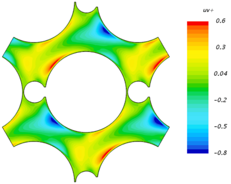

And many others

- ✓ 50 groups (incl. MIT, Stanford, Oxford, Imperial C., KTH, Chalmers, ...) in 15 countries
- ✓ In Code_Saturne (EDF, open-source)
- ✓ In CEDRE, AETHER
- ✓ In OpenFOAM
- ✓ In StarCCM+

Comparison with experiments

Velocity field

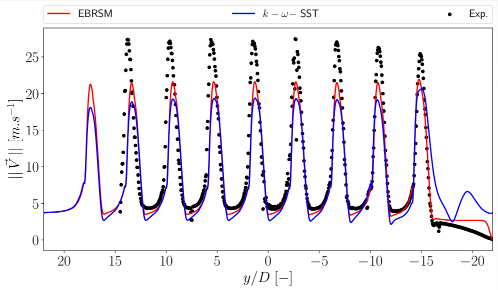

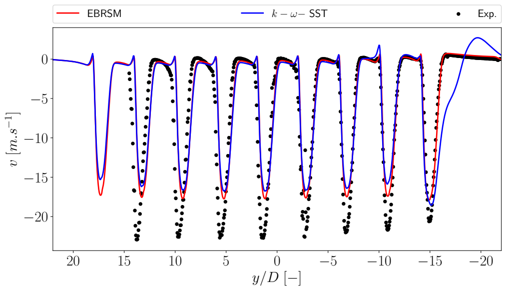

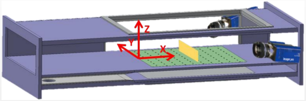

Profiles along the line above the first row, at $x = 3.05D$ and $z = 0.58D$

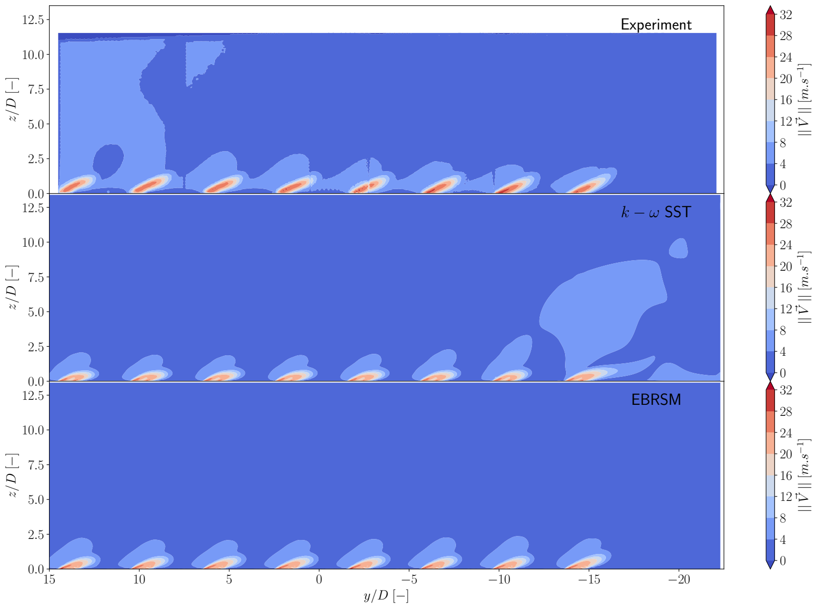

Isocontours of velocity magnitude in the plane $x/D = 0.305$ (row 1)

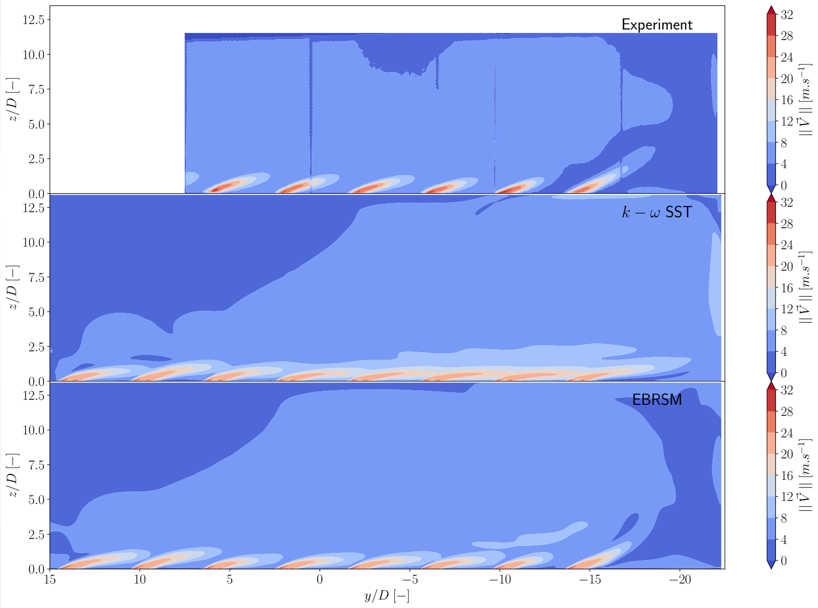

Isocontours of velocity magnitude in the plane $x/D = 1.165$ (row 3)

Temperature field

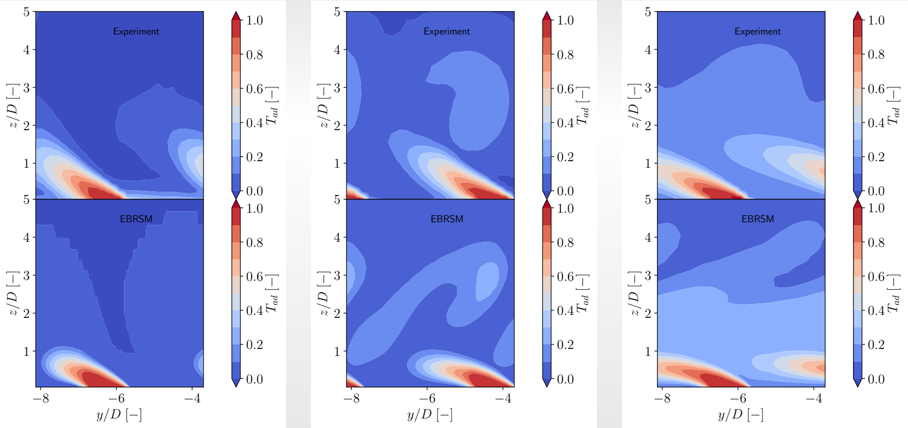

Non-dimensional temperature field in the planes
$x/D = 0.305$; 0.735; 1.165 (rows 1, 2 and 3)

Wall temperature

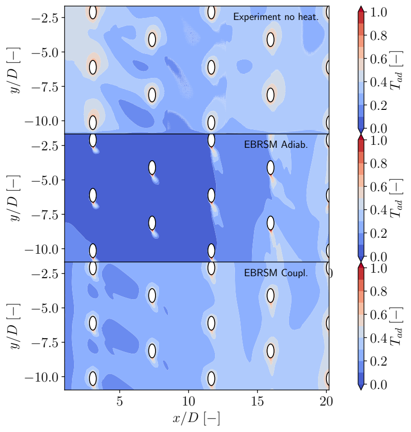

Upper surface of the plate.

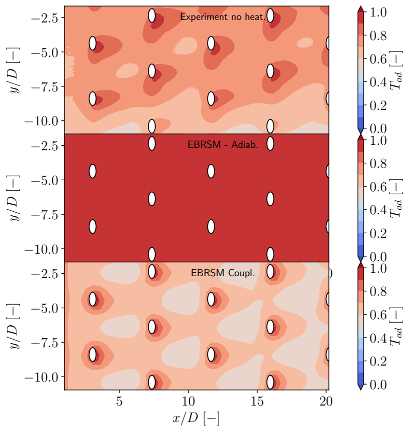

Lower surface of the plate.

Hybrid RANS-LES approach

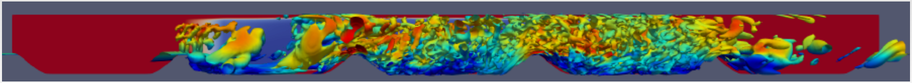

Example of a periodic hill flow

HTLES $\rightarrow$ k-ω–SST

$$\nu_{\text{sfs}} = \frac{k_{\text{sfs}}}{\psi_\omega(r)\,\omega^*_{\text{sfs}}} \qquad \left\{ \begin{aligned} \frac{Dk_{\text{sfs}}}{Dt} &= P_{k\text{sfs}} + D_{k\text{sfs}} - \frac{k_{\text{sfs}}}{T(r)} \\ \frac{D\omega^*_{\text{sfs}}}{Dt} &= \gamma_\omega \frac{\omega^*_{\text{sfs}}}{k_{\text{sfs}}} P_{\text{sfs}} + D^*_{\omega\text{sfs}} - \beta_\omega {\omega^*_{\text{sfs}}}^2 + C^*_{\omega\text{sfs}} \end{aligned} \right.$$

$$T_{\text{m}} = \frac{r}{\psi_\omega(r)} \frac{k}{C_\mu k_{\text{m}} \omega^*_{\text{m}}} \qquad \psi_w(r) = \frac{\beta_\omega}{C_\mu \gamma_\omega + r(\beta_\omega - C_\mu \gamma_\omega)}$$

Energy ratio: $$r = \frac{k_m}{k} = \frac{1}{\beta_0} \left(\frac{U_S}{\sqrt{k}} \right)^{2/3} \left(\omega_c \frac{k}{\varepsilon} \right)^{-2/3}$$

Cutoff frequency: $$\omega_c = \min \left[\frac{\pi}{dt}; \frac{U_S \pi}{\Delta} \right]$$

Model available in StarCCM+ under the name SRH

Square-sectioned cylinder

(Tran, Manceau, Perrin, Borée, and Nguyen)

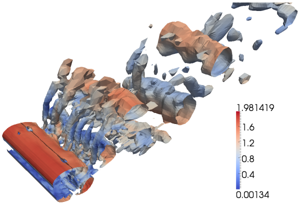

- ✓ $Re = 21400$
- ✓ Code_Saturne
- ✓ HTLES – k-ω–SST
- ✓ 0.5×10^6 cells

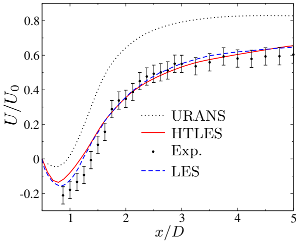

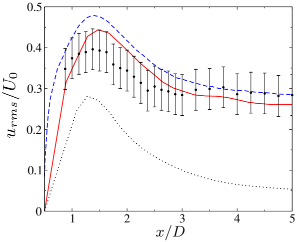

- ✓ Exp.: Lyn et al., 1995
- ✓ LES: Cao and Tamura, 2016 with 75×10^6 cells (factor 150)

Periodic hills

(Duffal2021b)

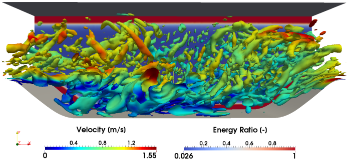

- ✓ $Re_b = 10600$
- ✓ Ref. LES by Breuer et al., 2006 with 12×10^6 cells
- ✓ Code_Saturne
- ✓ HTLES – k-ω–SST and HTLES – BL–$\overline{v^2}/k$
- ✓ M0=$160 \times 160 \times 80 = 2 \times 10^6$ cells (factor 6)
- ✓ M1=$80 \times 80 \times 40 = 256{,}000$ cells (factor 50)

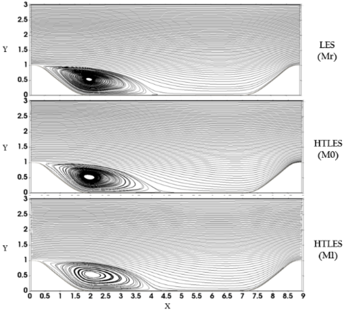

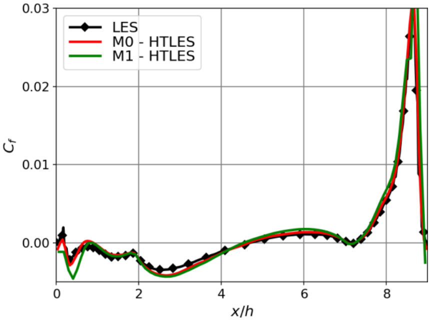

Simplified internal combustion engine

(Afailal et al., 2019)

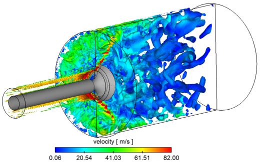

- ✓ Exp. by Dellenback et al., 1988
- ✓ Ref. LES by Thobois et al., 2004
- ✓ $Re_b = 30000$
- ✓ Code=*CONVERGE*
- ✓ HTLES – k-ω–SST
- ✓ 1.4×10^6 cells

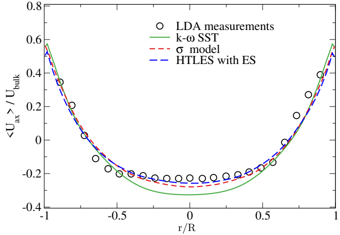

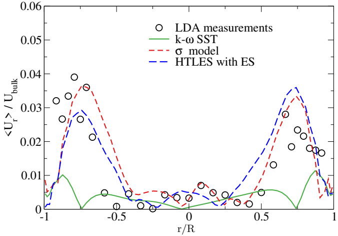

	EXP	RANS	HTLES	LES
ΔP [Pa]	1766	1713	1705	1957
Error [%]		-3	-3	+11

Single jet in crossflow

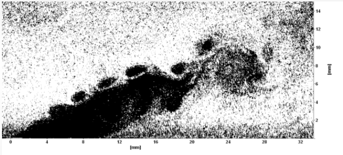

MAVERIC facility

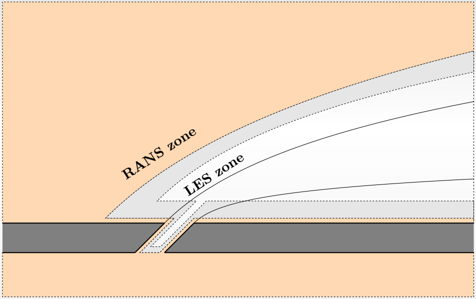

(Q-isocontours)

Acknowledgements

- ✓ Project funded by the H2020 project SOPRANO (grant agreement 690764) and the ASTURIES project (grant E2S-20-ScientificChallenges-01) of E2S UPPA (ANR-16-IDEX-0002).
- ✓ Simulation tool: Code_Saturne (Archambeau et al., 2004)
- ✓ Computing resources: MCIA, Bordeaux and GENCI-IDRIS (Grant 2022-A0122A10980).

Bibliography

Archambeau, F., N. Méchitoua, and M. Sakiz (2004). "Code Saturne: A Finite Volume Code for the Computation of Turbulent Incompressible flows - Industrial Applications". In: *Int. J. on Finite Volume, Electronical edition: http://averoes.math.univ-paris13.fr/html* ISSN 1634.0655.

Manceau, R., R. Perrin, M. Hadžiabdić, and S. Benhamadouche (2014). "Investigation of the interaction of a turbulent impinging jet and a heated, rotating disk". In: *Phys. Fluids* 26.3.

Lardeau, S. and R. Manceau (2014). "Computations of complex flow configurations using a modified Elliptic-Blending Reynolds-Stress model". In: *Proc. 10th ERCOFTAC Int. Symp. on Eng. Turb. Modelling and Measurements, Marbella, Spain.*

Benhamadouche, S., I. Afgan, and R. Manceau (2020). "Numerical simulations of flow and heat transfer in a wall bounded pin matrix". In: *Flow Turbul. Combust.* 104.1, pp. 19–44.

Borello, D., K. Hanjalic, and F. Rispoli (2005). "Prediction of cascade flows with innovative second-moment closures". In: *J. Fluid Eng.-T. ASME* 127.6, pp. 1059–1070.

Törnblom, O. and A. V Johansson (2007). "A Reynolds stress closure description of separation control with vortex generators in a plane asymmetric diffuser". In: *Phys. Fluids* 19.115108.

Dovizio, D., A. Shams, and F. Roelofs (2019). "Numerical prediction of flow and heat transfer in an infinite wire-wrapped fuel assembly". In: *Nucl. Eng. Des.* 349, pp. 193–205.

Tran, T.T., R. Manceau, R. Perrin, J. Borée, and A.T. Nguyen (2012). "A hybrid temporal LES approach. Application to flows around rectangular cylinders". In: *Proc. 9th ERCOFTAC Int. Symp. on Eng. Turb. Modelling and Measurements, Thessaloniki, Greece.*

Lyn, D.A., S. Einav, W. Rodi, and J.-H. Park (1995). "Laser-Doppler velocimetry study of ensemble-averaged characteristics of the turbulent near wake of a square cylinder". In: *J. Fluid Mech.* 304, pp. 285–319.

Cao, Y. and T. Tamura (2016). "Large-eddy simulations of flow past a square cylinder using structured and unstructured grids". In: *Comput. Fluids* 137, pp. 36–54.

Breuer, M., B. Jaffrézic, N. Peller, M. Manhart, J. Fröhlich, Ch. Hinterberger, W. Rodi, G.B. Deng, O. Chikhaoui, S. Jakirlić, et al. (2006). “A comparative study of the turbulent flow over a periodic arrangement of smoothly contoured hills”. In: *Direct and Large-Eddy Simulation VI*. Springer, pp. 635–642.

Afailal, H., J. Galpin, A. Velghe, and R. Manceau (2019). “Development and validation of a hybrid temporal LES model in the perspective of applications to internal combustion engines”. In: *Oil Gas Sci. Technol.* 74.56, p. 16.

Dellenback, P.A., D.E. Metzger, and G.P. Neitzel (1988). “Measurements in Turbulent Swirling Flow Through an Abrupt Axisymmetric Expansion”. In: *AIAA J.* 26.6.

Thobois, L., G. Rymer, T. Soulères, and T. Poinsot (2004). “Large-Eddy Simulation in IC Engine Geometries”. In: *2004 SAE Fuels & Lubricants Meeting & Exhibition*. SAE International.

Grid convergence study

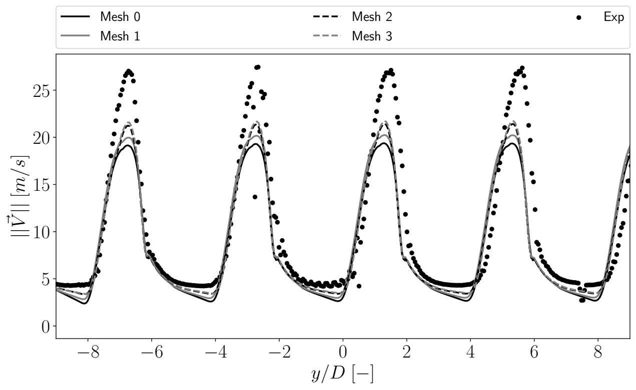

Figure: Velocity magnitude obtained with the k-ω-SST model extracted along the line above the first row, defined by $x = 3.05D$, at the elevation $z = 0.58D$, for the 4 meshes, compared with the experiments.